PCCP

PAPER

View Article Online
View Journal | View Issue

Cite this: *Phys. Chem. Chem. Phys.*, 2024, **26**, 5010

Liquid reagents are not enough for liquid assisted grinding in the synthesis of $[(AgBr)(n\text{-pica})]_n$†

Caterina Zuffa, [a] Chiara Cappuccino,‡[a] Lucia Casali, [ab] Franziska Emmerling [b] and Lucia Maini *[a]

Received 3rd October 2023,
Accepted 2nd January 2024

DOI: 10.1039/d3cp04791a

rsc.li/pccp

This study investigates the mechanochemical reactions between AgBr 3-picolylamine and 4-picolylamine. The use of different stoichiometry ratios of the reagents allows $[(AgBr)(n\text{-pica})]_n$ and $[(AgBr)_2(n\text{-pica})]_n$ to be obtained, and we report the new structures of $[(AgBr)_2(3\text{-pica})]_n$ and $[(AgBr)_2(4\text{-pica})]_n$ which are characterized by the presence of the following: (a) infinite inorganic chains, (b) silver atom coordinated only by bromide atoms and (c) argentophilic interactions. Furthermore, we studied the interconversion of $[(AgBr)(n\text{-pica})]_n$/$[(AgBr)_2(n\text{-pica})]_n$ by mechanochemical and thermal properties. The *in situ* experiments suggest that $[(AgBr)(3\text{-pica})]_n$ is kinetically favoured while $[(AgBr)_2(3\text{-pica})]_n$ is converted into $[(AgBr)(3\text{-pica})]_n$ only with a high excess of the ligand. Finally, the liquid nature of the ligands is not sufficient to assist the grinding process, and the complete reaction is observed with the addition of a small quantity of acetonitrile.

1. Introduction

Mechanochemistry, a field within the realm of chemistry, is dedicated to investigating the chemical and physicochemical alterations of substances in various states of aggregation induced by the impact of mechanical energy.[1,2] Although the grinding process has been known to induce transformation since the ancient times;[3–5] only over the past few decades, has mechanochemistry gained considerable momentum as an effective technique for conducting environmentally friendly and sustainable chemical synthesis.[1,6–9] The milling or grinding process activates the solid reagents in different ways such as by increasing the internal and surface energy, by expanding the surface area, and by reducing the coherence energy of the solids, allowing the reactions to occur[10] either during the grinding or after it has been completed.[11] Mechanochemical reactivity can be intentionally tuned by adding a catalytic amount of a liquid, usually a solvent, in particular when neat grinding alone fails to induce reactivity in certain systems.[1,7,12] The liquid-assisted grinding (LAG) method harnesses the power of a small amount of liquid component to stimulate, facilitate, or expedite the desired reactivity. In order to provide a precise and measurable description of LAG reactions, parameter η has been introduced[13,14] which is the ratio of the added liquid (in microliters) to the weight of solid reactants (in milligrams). The mechanical reactions in which one of the reagents is in liquid form are less common[15–19] and cannot be described using the η parameter since in such cases, the liquid phase can play a dual role, serving both as a reagent and aiding in the grinding process. Among the products that can be obtained through mechanochemistry, there are several metal-based ones, such as metal complexes,[20] MOFs[21–23] and coordination polymers.[24–28] The mechanochemical method is considerably simpler and faster compared to its solution-based counterparts, which are often solvothermal and require soluble metal reagents. A recently acknowledged advantage of mechanochemical reactivity is its remarkable ability to achieve precise stoichiometric control during the formation of products[24,29–32] and the possibility to obtain compounds which cannot be achieved by reactions in solution.[33,34] The products are generally obtained within a short time of grinding, such as 30–60 minutes,[35] and *in situ* experiments have shown a richness of intermediates during the formation of well-known compounds.[36] Despite extensive efforts,[37] our understanding of the fundamental mechanism underlying mechanochemical reactions remains incomplete.[38–41] This lack of comprehension poses significant limitations on our ability to fully leverage the potential of mechanochemistry and realize the transformative impact of this groundbreaking technology.[42] Solid-state reactions have been proven to be particularly efficient in the presence of a non-soluble reactant as in the case of CuX or AgX (X = halide), thus leading to new coordination polymers or hybrid coordination polymers not observed in conventional synthesis.[33,43,44]

[a] *Dipartimento di Chimica "G. Ciamician", Università di Bologna, Via F. Selmi 2, Bologna, Italy. E-mail: l.maini@unibo.it*
[b] *BAM Federal Institute for Materials Research and Testing, Richard-Willstätter-Strasse 11, 12489 Berlin, Germany*

† Electronic supplementary information (ESI) available. CCDC 2298748 and 2298749. For ESI and crystallographic data in CIF or other electronic format see DOI: https://doi.org/10.1039/d3cp04791a

‡ C.C. now at Chemistry Department, Brookhaven National Laboratory, Brookhaven, NY, USA.

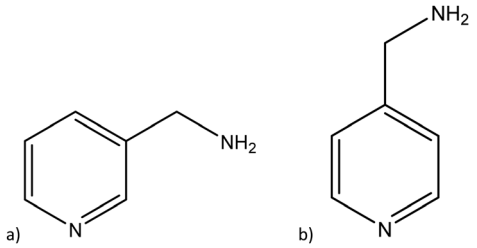

Scheme 1 (a) 3-Picolylamine (3-pica) and (b) 4-picolylamine (4-pica).

Coordination polymers based on copper(I) halide are studied for their luminescent, responsive, and conductive properties.[45–60]

Recently, we have reported a series of coordination polymers based on AgBr and picolylamine (pica hereafter) synthesized through mechanochemical reactions[43] which allowed us to avoid the problem of the limited solubility of AgBr[61] in commonly used solvents. Herein we explored the possibilities to obtain different compounds through the manipulation of stoichiometric ratios between the reactants. We successfully obtained two novel hybrid coordination polymers based on AgBr and 3- or 4-picolylamine referred to as 3- and 4-pica, respectively, see Scheme (1): $[(AgBr)_2(3\text{-pica})]_n$ and $[(AgBr)_2(4\text{-pica})]_n$ are characterized by argentophilic interactions, and the silver cations show a distance lower than 3.44 Å (hence inferior to the sum of the van der Waals radii).[62] On the basis of these results, we focused our attention on the investigation of the systems $[(AgBr)(3\text{-pica})]_n$/$[(AgBr)_2(3\text{-pica})]_n$ and $[(AgBr)(4\text{-pica})]_n$/$[(AgBr)_2(4\text{-pica})]_n$, and their interconversion using mechanochemical and thermal techniques. We explored which are the stoichiometry ratios that allow the formation of different pure compounds and how they interconvert. Moreover, we investigated the role of the liquid reagent; indeed picolylamines are liquid at room temperature and the synthesis can be described as a sort of LAG although it is not possible to determine the η value. The comparison of the experiments with or without the addition of acetonitrile confirmed the catalytic role of the solvent. Finally, direct *in situ* monitoring of the mechanochemical reactions *via* X-ray diffraction allowed us to detect the presence of an elusive intermediate and the appearance of the distinct phases, which helped us to understand the behaviour of the conversion.

2. Materials and methods

2.1. Synthetic procedures

All the reagents were purchased from Tokyo Chemical Industry (TCI). They were employed without additional purification, except for AgBr. AgBr was synthesized in the laboratory by utilizing an aqueous solution of $AgNO_3$ and saturated aqueous solution of NaBr. AgBr is solid and all the ligands (3- and 4-picolylamine, herein called 3 and 4-pica) are in the liquid phase. The synthesis of $[(AgBr)(n\text{-pica})]_n$ has been reported here.[43] Slurry synthesis is preferred to avoid the presence of unreacted AgBr.

2.2. Synthesis of $[(AgBr)_2(n\text{-pica})]_n$

Mechanochemical reaction (neat conditions). 1 mmol of AgBr (0.188 g) and 0.5 mmol of *n*-pica (0.05 mL) were placed in a 5 mL agate ball-milling jar with one agate sphere (5 mm diameter) and milled at 20 Hz for 60 minutes using a Retsch MM200 vibratory mill equipped with horizontally oscillating arms. The obtained crystalline powders were washed with acetonitrile to eliminate unreacted *n*-pica. In all cases unreacted AgBr was detected in XRPD despite washing several times. To explore the mechanochemical reaction of AgBr with 3-pica, 1 mmol of AgBr and different amounts of 3-pica (in the range of 0.1 mmol up to 3 mmol) were placed in a 5 mL agate ball-milling jar with one agate sphere (5 mm diameter) and milled at 20 Hz for 60 minutes using a Retsch MM200 vibratory mill equipped with horizontally oscillating arms. The obtained crystalline powders were not washed with acetonitrile to avoid further modification of the composition. The quantity of each phase of the powders was determined by Rietveld refinement and the data are summarized in Table S3 (ESI†).

LAG conditions. 1 mmol of AgBr (0.188 g), 0.5 mmol of 3-pica (0.05 mL) and 0.02 μL of acetonitrile (η = 0.1) were placed in a 5 mL agate ball-milling jar with one agate sphere (5 mm diameter) and milled at 20 Hz for 60 minutes using a Retsch MM200 vibratory mill equipped with horizontally oscillating arms. The obtained crystalline powders were washed with acetonitrile to eliminate unreacted *n*-pica. In this case unreacted AgBr is not detected. 1 mmol of AgBr (0.188 g) reacted with 1 mmol of *n*-pica (0.1 mL) and 0.02 μL of acetonitrile (η = 0.1) under the same conditions described before to obtain $[(AgBr)(3\text{-pica})]_n$. Also, in this case unreacted AgBr is not detected.

Slurry. 1 mmol of AgBr (0.188 g) and 0.5 mmol of *n*-pica (0.05 mL) were placed in a glass vessel with 1.5 mL of acetonitrile (η = 8) and the slurry was stirred in the dark (by covering the vessel with aluminium foil) for 24 hours. The crystalline powder was washed with acetonitrile. The XRPD patterns do not show unreacted AgBr.

Solvothermal reaction. 1 mmol of AgBr (0.188 g), 0.5 mmol of 3-pica (0.05 mL) and 2 mL of acetonitrile or THF were placed in a 5 mL glass vial and in a metal autoclave and placed in the stove at 90 °C for 24 hours. After that, the autoclave was cooled at 9 °C h^{-1} to reach room temperature. Single crystals of $[(AgBr)_2(3\text{-pica})]_n$ suitable for SCXRD were obtained. Solvothermal reactions with 4-pica were unsuccessful.

2.3. Conversion between $[(AgBr)(3\text{-pica})]_n$ and $[(AgBr)_2(3\text{-pica})]_n$

Mechanochemical conversion from the 1 : 1 phase to the 2 : 1 phase. 1 mmol of $[(AgBr)(3\text{-pica})]_n$ (0.296 g) and 1 mmol of AgBr (0.188 g) were added to a 5 mL agate ball-milling jar with one agate sphere with a diameter of 5 mm. The reactants were milled at 20 Hz for 60 minutes using a Retsch MM200 vibratory mill equipped with horizontally oscillating arms. The crystalline powders obtained were analysed by XRPD and show a complete conversion from $[(AgBr)(3\text{-pica})]_n$ to $[(AgBr)_2(3\text{-pica})]_n$, with the presence of unreacted AgBr.

Mechanochemical conversion from the 2 : 1 phase to the 1 : 1 phase. 1 mmol of $[(AgBr)_2(3\text{-pica})]_n$ (0.484 g) and from 1 to 2 mmol of 3-pica (0.1–0.2 mL) were added to a 5 mL agate ball-milling jar with one agate sphere with a diameter of 5 mm. The reactants were milled at 20 Hz for 60 minutes using a Retsch MM200 vibratory mill equipped with horizontally oscillating arms. The crystalline powders obtained were analysed by XRPD. The powder obtained by adding 1 mmol of 3-pica does not show a complete conversion and is a mixture of $[(AgBr)_2(3\text{-pica})]_n$ and $[(AgBr)(3\text{-pica})]_n$; the complete conversion from the 2 : 1 phase to the 1 : 1 phase was observed when 2 mmol of 3-pica was used. No presence of unreacted AgBr has been detected.

Thermal conversion. The thermal conversion was observed by hot stage microscopy. Crystals of $[(AgBr)(3\text{-pica})]_n$ were heated at 10 °C min^{-1}; the release of the ligand and conversion into $[(AgBr)_2(3\text{-pica})]_n$ were observed at around 65 °C, while the melting was observed at 106 °C.

Thermal conversion. The powder of $[(AgBr)(3\text{-pica})]_n$ was heated at 65 °C for 2 hours and analysed by XRPD. The analysis showed a complete conversion to $[(AgBr)_2(3\text{-pica})]_n$, with the presence of AgBr.

2.4. Conversion between $[(AgBr)(4\text{-pica})]_n$ and $[(AgBr)_2(4\text{-pica})]_n$

Mechanochemical conversion from the 1 : 1 phase to the 2 : 1 phase. 1 mmol of $[(AgBr)(4\text{-pica})]_n$ (0.296 g) and 1 mmol of AgBr (0.188 g) were added to a 5 mL agate ball-milling jar with one agate sphere with a diameter of 5 mm. The reactants were milled at 20 Hz for 60 minutes using a Retsch MM200 vibratory mill equipped with horizontally oscillating arms. The crystalline powders obtained were analysed by XRPD and show a mixture of $[(AgBr)_2(4\text{-pica})]_n$ and $[(AgBr)(4\text{-pica})]_n$. A complete conversion from $[(AgBr)(4\text{-pica})]_n$ to $[(AgBr)_2(4\text{-pica})]_n$ was obtained by adding 0.02 mL of acetonitrile before grinding.

Mechanochemical conversion from the 2 : 1 phase to the 1 : 1 phase. 1 mmol of $[(AgBr)_2(4\text{-pica})]_n$ (0.484 g) and 1 mmol of 4-pica (0.1 mL) were added to a 5 mL agate ball-milling jar with one agate sphere with a diameter of 5 mm. The reactants were milled at 20 Hz for 60 minutes using a Retsch MM200 vibratory mill equipped with horizontally oscillating arms. The crystalline powders obtained were analysed by XRPD and correspond to the 1 : 1 phase.

2.5. Structure determination by single crystal

The single crystal data of $[(AgBr)_2(3\text{-pica})]_n$ were collected at room temperature on an Oxford Xcalibur using Mo-Kα radiation, equipped with a graphite monochromator and a CCD Sapphire detector. Crystal data details are summarized in Table 1 (see also Table S1 in the ESI†). The SHELXT[63] and SHELXL[64] algorithms were used for the solution and refinement of the structures based on F^2. All the atoms, excluding the hydrogens, were refined anisotropically. Hydrogen atoms have been added to the theoretical positions. The principal crystallographic data are reported in Table 1.

Table 1 Crystal data and structure refinement for $[(AgBr)_2(n\text{-pica})]_n$ coordination polymers. $[(AgBr)_2(4\text{-pica})]_n$ was determined by XRPD

	$[(AgBr)_2(3\text{-pica})]_n$	$[(AgBr)_2(4\text{-pica})]_n$
Empirical formula	$C_6H_8Ag_2Br_2N_2$	$C_6H_8Ag_2Br_2N_2$
Formula weight (g mol^{-1})	483.68	483.68
T (K)	293	293
Wavelength (Å)	0.71073	1.535
Crystal system	Monoclinic	Orthorhombic
Space group	$C2/c$	$Pbca$
a (Å)	24.605(3)	14.282(1)
b (Å)	6.2851(5)	22.011(1)
c (Å)	14.3050(12)	6.624(1)
β (°)	110.938(9)	90
V (Å^3)	2066.2(3)	2082
Z, Z'	8, 1	8, 1
GoF on F^2	0.991	1.08
R_1 [$I > 2\sigma(I)$] or R_p	0.0726	0.0448
wR_2 (all data) or R_{wp}	0.1277	0.0607

2.6. Structure determination by powder X-ray diffraction

The structure of $[(AgBr)_2(4\text{-pica})]_n$ was solved by X-ray powder diffraction. The powder data were obtained on a Panalytical X'Pert PRO using Cu-kα radiation, endowed with micro-focusing, a pixel detector and a capillary holder. The sample was loaded in a 0.5 mm glass capillary. The analysis was conducted in transmission and collected in the 2θ range of 5–75°, with 0.02 rad soller, 1/4° divergence slit and 1/4° antiscatter slit, step size 0.0131° and a counting time of 128 520 s. Six consecutive repetitions of the same measurement were collected and merged to obtain an optimal ratio between the signal and the noise. The analysis of the powder data was performed using the software TOPAS 6;[65] a Chebyshev function and a pseudo-Voigt (TCHZ type) were used to fit the background and the peak shape, respectively. The powders were indexed with the cell reported in Table 1. The structure was determined by simulated annealing and refined by the Rietveld method. The principal crystallographic data are reported in Table 1.

CCDC 2298748 and 2298749 contain the supplementary crystallographic data for this paper. The data can be obtained free of charge from The Cambridge Crystallographic Data Centre *via* www.ccdc.cam.ac.uk/structures. The graphical representations of the structures were displayed using the software MERCURY.[66]

2.7. Rietveld quantitative analysis

The powder patterns were refined using the Rietveld method with X'Pert HighscorePlus V4.9[67] suite. A Chebyshev function and a pseudo-Voigt (TCHZ type) were employed to fit the background and the peak shape, respectively. To account for preferred orientation, the spherical harmonics correction was applied.

2.8. Thermogravimetric analysis (TGA)

Thermogravimetric analyses were performed using a PerkinElmer TGA7 instrument. The measurements were carried out under nitrogen flow in a temperature range of 30–350 °C with a 5 °C min^{-1} gradient.

2.9. Differential scanning calorimetry (DSC)

DSC: calorimetric measurements were performed with a PerkinElmer Diamond DSC-7 equipped with a PII intracooler. The temperature and enthalpy calibrations were performed with a high purity standard (*n*-decane, benzene and indium). The samples in aluminum open pans were heated at 10 °C min^{-1} unless otherwise indicated.

2.10. Hot stage microscopy (HSM)

The analysis was performed using an OLYMPUS BX41 microscope equipped with a VISICAM 5.0 camera and a system for the temperature control Linkam TMS 94. The photos were taken under polarized light to underline the modification due to solid state transition, with a 100× magnification.

2.11. Time resolved *in situ* analysis (TRIS)

In situ X-ray diffraction measurements were performed at 10 s intervals at the μSpot beamline (BESSY II, Helmholtz Centre Berlin for Materials and Energy).[68] The reactions were carried out in a vibrational ball mill (Pulverisette 23, Fritsch, Germany) using a custom-made Perspex grinding jar of 12 mm diameter.[69] The experiments were conducted with a wavelength of 0.7314 Å using a double crystal monochromator (Si 111). The obtained scattering images were integrated using the Dpdak-software[70] and background corrected using a python script.

Synchrotron experiments for *in situ* monitoring. The mechanochemical reactions between AgBr and 3-pica were performed at 50 Hz in a vibration ball mill (Pulverisette 23, Fritsch, Germany) in a Perspex jar with plastic caps (12 mm diameter) using an 8 mm agate ball as follows: (1) NG (neat grinding) of 2AgBr (0.1878 g) and 3-pica (0.05 mL) for 1 hour; (2) NG of AgBr (0.0469 g) and 3-pica (0.025 mL) 1 hour.

3. Results and discussion

3.1. Crystal structure of $[(AgBr)(3\text{-pica})]_n$ (1 : 1 phase)

The crystalline structure of $[(AgBr)(3\text{-pica})]_n$ has already been published,[43] and here we report only the main information for sake of clarity. The silver and bromine atoms form a single chain along the screw axis, and the tetrahedral coordination of the silver atom is fulfilled by two 3-pica molecules that coordinate the metal centre with the pyridine and the amine nitrogen atoms, respectively (Fig. 1). The organic ligands bridge the inorganic chains forming a 2-D network.

3.2. Crystal structure of $[(AgBr)_2(3\text{-pica})]_n$ (2 : 1 phase)

The crystalline structure of $[(AgBr)_2(3\text{-pica})]_n$ was determined using single crystal X-ray diffraction (SCXRD) analysis. A colourless, rectangular crystal was obtained through a solvothermal reaction. The silver bromine atoms form a distinctive infinite network which has been previously described in the literature in a coordination polymer of AgX (X = Br, Cl) and quinoline, and the inorganic component is referred to as a "saddle polymer".[71,72] In the asymmetric unit, three different silver atoms are present: Ag1 is in the general position and Ag2 and Ag3 lie on the 2-fold axis (and hence with half occupancy) while the two bromide ions are in general positions (Fig. 2). The Ag1 atom achieves tetrahedral coordination by binding two bromine atoms and two ligands, and it is 3.244 Å from Ag3. On the other hand, Ag2 and Ag3 atoms solely coordinate with bromine atoms, giving them a purely inorganic character. Notably, Ag2 and Ag3 are positioned on the 2-fold axis and exhibit short Ag–Ag distances of 3.072 Å and 3.214 Å, consistent with argentophilic interactions,[62] resulting in the formation of an infinite and linear wire of silver cations. The organic ligands bridge the inorganic chains forming 2-D networks as shown in Fig. 2b and c.

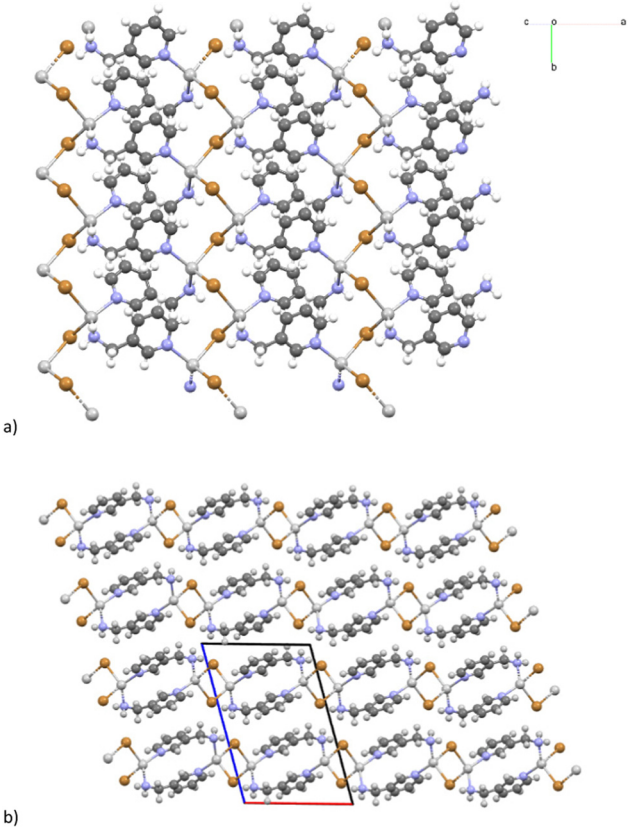

Fig. 1 Structure of $[(AgBr)(3\text{-pica})]_n$.[43] (a) Single chains of AgBr bridged by the organic ligands; (b) packing along the *b*-axis. All the "chains" are parallel within and among the layers due to the $P2_1$ space group. Cell axis colour: a is red, b is green, and c is blue.

3.3. Crystal structure of $[(AgBr)(4\text{-pica})]_n$ (1 : 1 phase)

The crystalline structure of the 1 : 1 phase, $[(AgBr)(4\text{-pica})]_n$, has been recently published.[43] The structure is characterized by the presence of a dimer of AgBr with an Ag–Ag distance of 3.198 Å. The organic ligands bridge the dimer forming a 2-D network (Fig. 3). The corrugated layers run parallel to each other.

3.4. Crystal structure of $[(AgBr)_2(4\text{-pica})]_n$

The crystalline structure of $[(AgBr)_2(4\text{-pica})]_n$ was determined by powder X-ray diffraction (PXRD) of a crystalline powder obtained through ball milling. The asymmetric unit consists

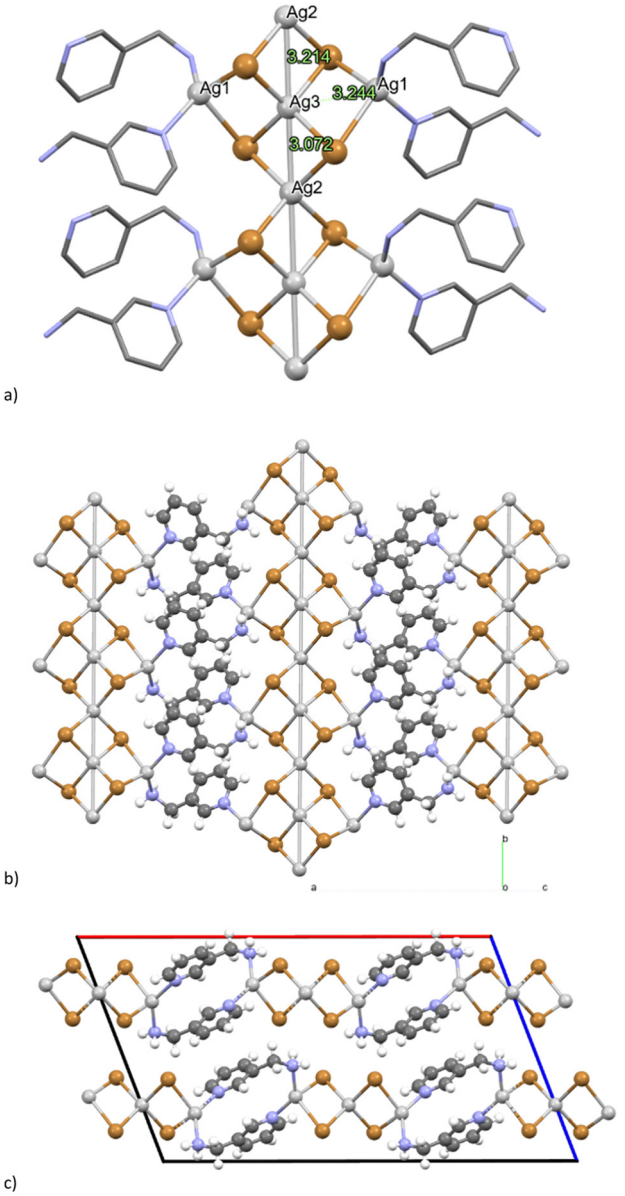

Fig. 2 (a) Inorganic saddle chain; (b) 2-D network with the inorganic chain parallel to the *b* axis and (c) packing along the *b*-axis of $[(AgBr)_2(3\text{-pica})]_n$. Cell axis color: *a* is red, *b* is green, and *c* is blue.

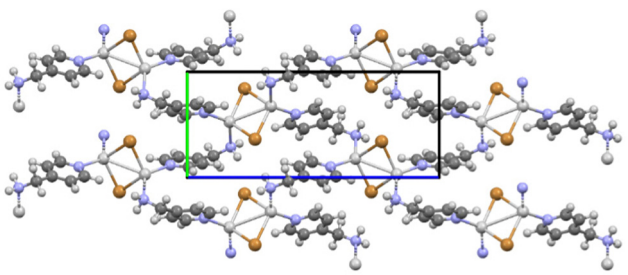

Fig. 3 Packing along the *a*-axis of $[(AgBr)(4\text{-pica})]_n$.[43] Cell axis color: *a* is red, *b* is green, and *c* is blue.

of two bromide ions and two silver atoms and one organic ligand. The metal and halide atoms form an infinite structure which is reminiscent of a distorted saddle (Fig. 4). Ag1 is coordinated with two bromide atoms and amine and pyridine nitrogen atoms, belonging to two different ligands, that bridge the inorganic chains forming a 2D network. Ag2, on the other hand, forms connections with four bromide atoms, leading to a complete inorganic coordination environment. The structure presents short Ag–Ag contacts, 2.979 Å and 3.138 Å, indicative of an argentophilic interaction among the central silver atom

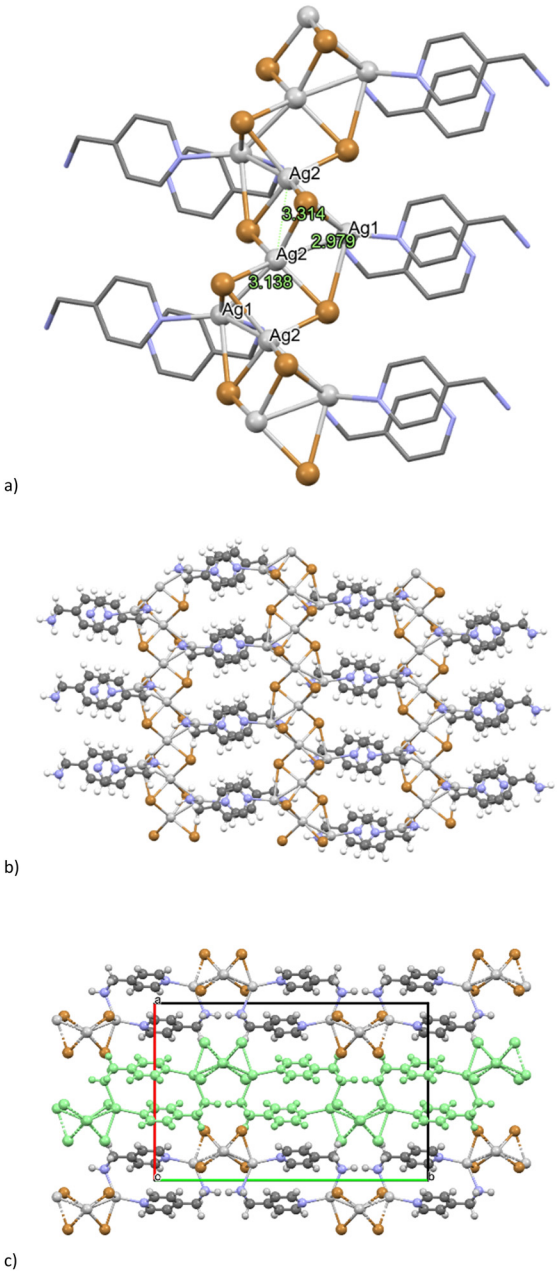

Fig. 4 Crystal structure of $[(AgBr)_2(4\text{-pica})]_n$. (a) Inorganic distorted saddle chain highlighting the distances among the silver atoms; (b) the 2-D layer with the ligands bridging the inorganic chains. The inorganic chain is parallel to the *c* axis. (c) Packing along the *c*-axis, showing three layers. The central layer is coloured in light green. Cell axis colour: *a* is red, *b* is green, and *c* is blue.

(Ag2) and the side ones (Ag1), and a longer contact (3.314 Å) among the Ag2 silver atoms, but still in the range of argentophilic interactions.

3.5. Thermal analysis. The DSC analysis of $[(AgBr)(3\text{-pica})]_n$ (**Fig. S2** in the ESI†) exhibits two endothermic peaks at 65 °C and 108 °C, indicating two distinct events. The peak at 65 °C corresponds to the release of the 3-pica ligand (consistent with the TGA analysis published here[43] in the ESI†) and formation of $[(AgBr)_2(3\text{-pica})]_n$ which melts at 108 °C. The conversion from the 1 : 1 phase to the 2 : 1 phase was confirmed also by XRPD of the powder of $[(AgBr)(3\text{-pica})]_n$ annealed at 65 °C for 15 minutes. The DSC analysis of $[(AgBr)_2(3\text{-pica})]_n$ (**Fig. S3, ESI**†) shows only the melting point at 106 °C comparable with the melting point observed previously.

To provide a comprehensive understanding of the phenomenon, the conversions were also observed in hot stage microscopy analysis. The phase transition initiates at approximately 65 °C, and by 80 °C, it is fully completed. At 106 °C, the compound undergoes complete melting (Fig. 5).

3.6. *In situ* and *ex situ* mechanochemical syntheses of $[(AgBr)(3\text{-pica})]_n$ and $[(AgBr)_2(3\text{-pica})]_n$ and their interconversion

As observed for several systems,[27,38,44] merely combining the reagents, AgBr and 3-pica, in precise stoichiometric quantities, is insufficient to react completely the reagents, both through slurry and mechanochemical syntheses, as the presence of AgBr was always observed. To obtain a more comprehensive understanding of the $[(AgBr)(3\text{-pica})]_n/[(AgBr)_2(3\text{-pica})]_n$ system, we synthetized the products maintaining a constant AgBr quantity (1 mmol) with a variable quantity of 3-pica from 0.1 up to 3 mmol and observed the different ranges of stability of the two compounds. All the reactions were run in the ball mill for 60 min to reach the conditions of steady state. Afterward, the resulting powders were analysed *via* X-ray analysis, followed by a Rietveld refinement to determine the respective proportions in mass of each phase present in the final powder (see Table S3 in ESI†).

As depicted in Fig. 6, the presence of $[(AgBr)_2(3\text{-pica})]_n$ (2 : 1 phase) in the synthesis products increases until it reaches a maximum and then gradually diminishes until it vanishes. The maximum is attained when the 3-pica is slightly in excess, precisely at a stoichiometric ratio of 1 : 0.6 with the presence of about ∼3% of unreacted AgBr. When 0.7 mmol of 3-pica is added to silver bromide, $[(AgBr)(3\text{-pica})]_n$ starts to appear, and the powder is a mixture of the 1 : 1 and 2 : 1 phases with still some unreacted AgBr. By increasing the amount of ligand in the reaction, the formation of $[(AgBr)(3\text{-pica})]_n$ is favoured, but with the ratio of 1 : 1.5 (AgBr : 3-pica) only $[(AgBr)(3\text{-pica})]_n$ is formed but still some unreacted AgBr is present. The silver bromide fully reacts only in the presence of a great excess of the organic ligand (3 mmol). We explored the possibility to increase the yield of the reaction by adding 0.02 mL of acetonitrile and we selected the reaction which gave pure phases but still unreacted salt. In both cases (1 : 0.6 and 1 : 1.5) the presence of acetonitrile allowed the completeness of the reaction to be reached and the desired compound $[(AgBr)_2(3\text{-pica})]_n$ and $[(AgBr)(3\text{-pica})]_n$ to be obtained, respectively. It is not possible to draw a general conclusion, but the role of acetonitrile is not merely for the presence of a liquid during the milling, since pica is liquid itself, neither as a solvent of the insoluble AgBr. In fact, the organic ligand is a better solvent of the salt than acetonitrile, because of its higher coordination power. It is true that the presence of the acetonitrile diminishes the viscosity of picolyamine and improves the mixing of the powder and thus catalyzes the reaction.

We also conducted time resolved *in situ* measurements (TRIS) at the synchrotron to enhance our understanding of the events taking place during the grinding process. When the AgBr and 3-pica reagents are mixed in a precise stoichiometric ratio of 2 : 1, in the initial 10 minutes we observed a transient

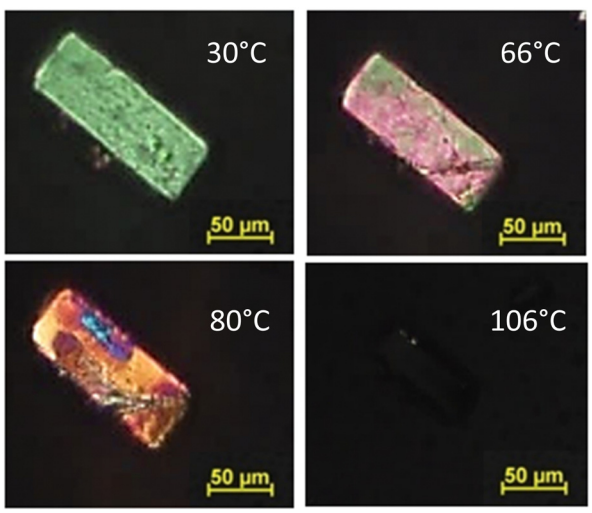

Fig. 5 $[(AgBr)(3\text{-pica})]_n$ crystal at 30 °C, 66 °C during the phase transition, 80 °C phase transition completed, and 106 °C completely melted.

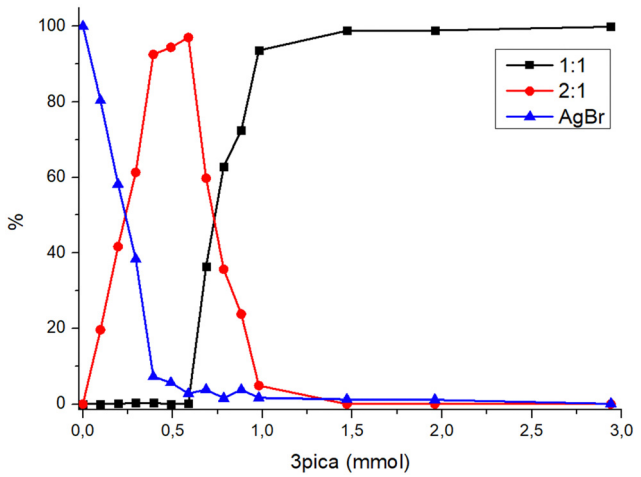

Fig. 6 Composition in mass of the powders derived from grinding AgBr for 60 minutes (constant amount of 1 mmol) with different aliquots of 3-pica; the weight mass percentages of the 1 : 1 phase in black, 2 : 1 phase in red, and AgBr phase in blue.

peak which gradually subsides, concomitant with the peaks of $[(AgBr)(3\text{-pica})]_n$, and the desired $[(AgBr)_2(3\text{-pica})]_n$ (see Fig. 7). The peaks of $[(AgBr)(3\text{-pica})]_n$ partially faded with a prolonged grinding without disappearing. As observed in an *ex situ* experiment a small fraction of AgBr remains unreacted (see ESI†). It is worth noting that the *in situ* experiments are carried out in different vials and with a vertical vibration, which can lead to a different result compared to the *ex situ* experiments.

When the reagents are mixed in a stoichiometric ratio of 1 : 1, we observed a transient peak at 4.2 nm^{-1} for the initial two minutes, a similar situation to the previous case, followed by the rapid formation of the 1 : 1 phase. After 10 minutes, the 2 : 1 phase appears and persists yielding at the end of the measurements to a mixture of 1 : 1 and 2 : 1 phases (Fig. 8).

These data suggest that the 1 : 1 phase is kinetically favoured, as it exclusively forms during the initial minutes of the reaction. However, the appearance of the 2 : 1 phase afterwards suggests that $[(AgBr)_2(3\text{-pica})]_n$ is favoured when the pica ligand is not in excess. These considerations allowed the understanding of the conversion of the two compounds by mechanochemical synthesis.

In fact, it is possible to obtain $[(AgBr)_2(3\text{-pica})]_n$ by grinding $[(AgBr)(3\text{-pica})]_n$ with the required amount of AgBr. However, to achieve complete conversion from the $[(AgBr)_2(3\text{-pica})]_n$ phase into the $[(AgBr)(3\text{-pica})]_n$ *via* mechanochemistry, a substantial excess of the ligand (twice the stoichiometric ratio) must be added (refer to the ESI†). The possibility to obtain pure $[(AgBr)(3\text{-pica})]_n$ with only a slight excess of 3-picolylamine is clarified by the *in situ* experiment; the 1 : 1 phase is first

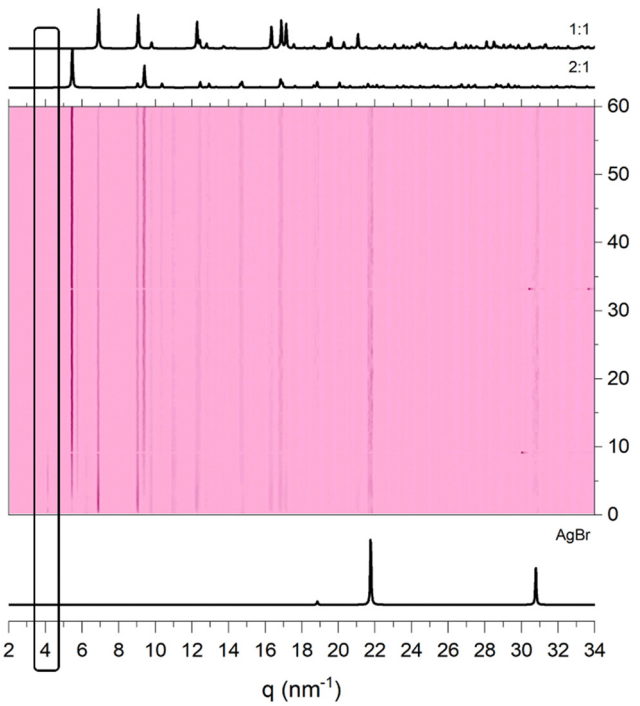

Fig. 7 TRIS (time-resolved *in situ*) analysis of AgBr and 3-pica mixed in a 2 : 1 stoichiometric ratio. The transient peak at 4.2 nm^{-1} in the first minutes is highlighted.

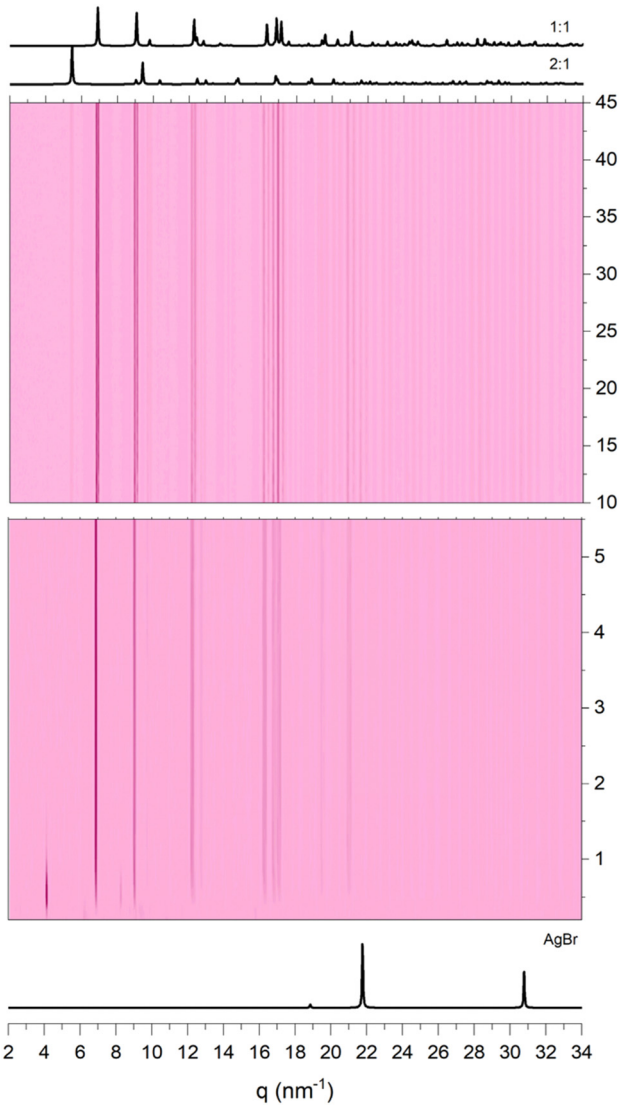

Fig. 8 TRIS analysis of AgBr and 3-pica mixed in a 1 : 1 stoichiometric ratio.

obtained and if there is enough ligand in excess it does not convert into the 2 : 1 phase; on the other hand, the stability of $[(AgBr)_2(3\text{-pica})]_n$, once obtained, prevents its conversion.

3.7. Mechanochemical synthesis of $[(AgBr)(4\text{-pica})]_n$ and $[(AgBr)_2(4\text{-pica})]_n$ and their interconversion

The synthesis of $[(AgBr)(4\text{-pica})]_n$ and $[(AgBr)_2(4\text{-pica})]_n$ can be easily achieved by grinding AgBr and 4-pica in the desired stoichiometric ratio and a small amount of acetonitrile to avoid the presence of unreacted silver bromide. While no phase transitions were observed in the DSC analysis of $[(AgBr)(4\text{-pica})]_n$, we investigated the possibility of converting $[(AgBr)(4\text{-pica})]_n$ into $[(AgBr)_2(4\text{-pica})]_n$ and *vice versa* through mechanochemical reactions. Interestingly, by adding the stoichiometric quantity of 4-pica to $[(AgBr)_2(4\text{-pica})]_n$ it converts into $[(AgBr)(4\text{-pica})]_n$ and a small fraction of AgBr is detected. The complete conversion and the pure $[(AgBr)(4\text{-pica})]_n$ phase

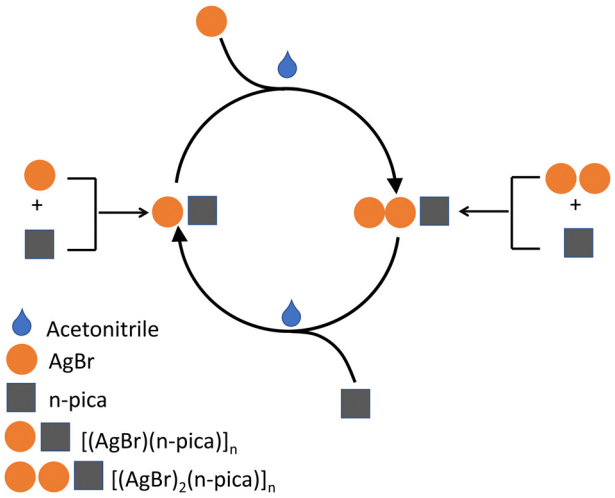

Fig. 9 Summary scheme of the mechanochemical reactions to obtain $[(AgBr)(n\text{-pica})]_n$ and $[(AgBr)_2(n\text{-pica})]_n$ and their interconversions.

are obtained by the addition of the required amount of 4-pica along with the use of acetonitrile. On the other hand, by adding the stoichiometric amount of silver bromide to $[(AgBr)(4\text{-pica})]_n$ a mixture of the 1 : 1 and 2 : 1 phases is obtained, the complete conversion can be achieved by adding 0.02 mL of acetonitrile to the reaction (Fig. 9).

4. Conclusions

The mechanochemical synthesis of AgBr and the *n*-pica led to the two different compounds $[(AgBr)_2(n\text{-pica})]_n$ and $[(AgBr)(n\text{-pica})]_n$ depending on the stoichiometric ratio. The structures of $[(AgX)(n\text{-pica})]_n$ are not isostructural and present a different connectivity of the inorganic part. While $[(AgBr)(3\text{-pica})]_n$ is characterized by the presence of single chains of AgBr, the analogous compound with 4-pica is characterized by the presence of Ag_2Br_2 dimers. The structure of $[(AgBr)_2(n\text{-pica})]_n$ has been determined by single crystal and powder X-ray diffraction of 3-pica and 4-pica, respectively. Although they are not isostructural, they show several features in common, like the presence of infinite inorganic chains, the presence of silver atoms coordinated only by bromide atoms and the presence of argentophilic interactions. These features make the hybrid coordination polymers $[(AgBr)_2(n\text{-pica})]_n$ interesting for conductive properties, which we are investigating. It is worth noting that our studies on AgXL including also these two new compounds, revealed that 88% of $[(AgX)_m(n\text{-pica})]_n$ (where X = Br^-, I^- and m = 1, 2) are hybrid coordination polymers, a percentage significantly higher than the 16% observed in the CSD[73] research.[43] This remarkable difference raises questions about the potential bias in the data from the CSD, which might be influenced by the prevalent use of solution-based synthetic procedures for the crystal structure solution. Historically, solution-based reactions have been favoured, but the low solubility of AgX salts limits the formation of the desired products, leading to a reduced number of structures in the database. The mechanochemical synthesis, as employed in our study, has proven to be advantageous for achieving a higher number of compounds with different stoichiometries. Through the implementation of *in situ* and *ex situ* studies, we gained valuable insights into key aspects of the mechanochemical process. Specifically, for the compounds with 3-pica, $[(AgBr)(3\text{-pica})]_n$ is observed from the very beginning of the reaction regardless of the amount of 3-pica used, revealing this phase to be kinetically favoured. Additionally, the presence of a transient phase was observed, although its determination was challenging. On the other hand, $[(AgBr)_2(3\text{-pica})]_n$ appears to be particularly stable, and it can be easily obtained by direct synthesis of AgBr and the 3-pica, by thermal decomposition of $[(AgBr)(3\text{-pica})]_n$ or by grinding $[(AgBr)(3\text{-pica})]_n$ with the correct amount of AgBr. The reactions of AgBr with different amounts of 3-pica allowed the detection of the correct ratio of reagents to gain the highest yield and to isolate the pure phases. The comparison of the grinding process with or without the addition of acetonitrile confirmed the catalytic role of the solvent. Hence, although a liquid reagent is present, the term LAG should be used only when the reaction is carried out in the presence of acetonitrile whose catalytic role has been demonstrated. In fact, the presence of the liquid reagent is not sufficient to lead the reaction to completeness, and unreacted AgBr was observed also in the presence of a large excess of 3-pica, while the addition of a small quantity of acetonitrile allowed the complete reaction of AgBr. The catalytic role of acetonitrile was also observed in the mechanochemical synthesis of $[(AgBr)(4\text{-pica})]_n$ and $[(AgBr)_2(4\text{-pica})]_n$. The conversion between these two compounds can be easily achieved by grinding, whereas the thermal treatment leads only to the melting of the compounds.

Author contributions

Conceptualization and methodology: L. M.; sample preparation: C. C. and C. Z.; experiments and data evaluation: C. C., C. Z., and L. C.; data analysis: all authors; writing: all authors. All authors have read and agreed to the published version of the manuscript.

Conflicts of interest

There are no conflicts to declare.

Acknowledgements

This work benefited from the networking activities carried out within the EU-funded COST Action CA18112–Mechanochemistry for Sustainable Industry.

References

1 J. L. Do and T. Friščić, *ACS Cent. Sci.*, 2017, **3**, 13–19.
2 T. E. Fischer, *Ann. Rev. Mater. Sci.*, 1988, **18**, 303–323.

3 M. Marchini, M. Gandolfi, L. Maini, L. Raggetti and M. Martelli, *Proc. Natl. Acad. Sci. U. S. A.*, 2022, **119**, 1–8.
4 L. Takacs, *JOM*, 2000, **52**, 12–13.
5 L. Takacs, *Chem. Soc. Rev.*, 2013, **42**, 7649–7659.
6 S. L. James, C. J. Adams, C. Bolm, D. Braga, P. Collier, T. Frišcic, F. Grepioni, K. D. M. Harris, G. Hyett, W. Jones, A. Krebs, J. Mack, L. Maini, A. G. Orpen, I. P. Parkin, W. C. Shearouse, J. W. Steed and D. C. Waddell, *Chem. Soc. Rev.*, 2012, **41**, 413–447.
7 D. Tan and F. García, *Chem. Soc. Rev.*, 2019, **48**, 2274–2292.
8 A. M. Belenguer, T. Friščić, G. M. Day and J. K. M. Sanders, *Chem. Sci.*, 2011, **2**, 696–700.
9 J.-L. Do and T. Friščić, *ACS Cent. Sci.*, 2016, **3**, 13–19.
10 D. Braga, F. Grepioni, L. Maini and S. d'Agostino, *Eur. J. Inorg. Chem.*, 2018, 3597–3605.
11 P. Baláž, A. Aláčová, M. Achimovičová, J. Ficeriová and E. Godočíková, *Hydrometallurgy*, 2005, **77**, 9–17.
12 A. M. Belenguer, G. I. Lampronti, A. J. Cruz-Cabeza, C. A. Hunter and J. K. M. Sanders, *Chem. Sci.*, 2016, **7**, 6617–6627.
13 T. Friščić, S. L. Childs, S. A. Rizvi and W. Jones, *CrystEngComm*, 2009, **11**, 418–426.
14 P. Ying, J. Yu and W. Su, *Adv. Synth. Catal.*, 2021, **363**, 1246–1271.
15 S. Hwang, S. Grätz and L. Borchardt, *Chem. Commun.*, 2022, **58**, 1661–1671.
16 P. P. Mazzeo, C. Carraro, A. Monica, D. Capucci, P. Pelagatti, F. Bianchi, S. Agazzi, M. Careri, A. Raio, M. Carta, F. Menicucci, M. Belli, M. Michelozzi and A. Bacchi, *ACS Sustainable Chem. Eng.*, 2019, **7**, 17929–17940.
17 F. Montisci, P. P. Mazzeo, C. Carraro, M. Prencipe, P. Pelagatti, F. Fornari, F. Bianchi, M. Careri and A. Bacchi, *ACS Sustainable Chem. Eng.*, 2022, **10**, 8388–8399.
18 O. Shemchuk, S. D'Agostino, C. Fiore, V. Sambri, S. Zannoli, F. Grepioni and D. Braga, *Cryst. Growth Des.*, 2020, **20**, 6796–6803.
19 C. Fiore, I. Sovic, S. Lukin, I. Halasz, K. Martina, F. Delogu, P. C. Ricci, A. Porcheddu, O. Shemchuk, D. Braga, J. L. Pirat, D. Virieux and E. Colacino, *ACS Sustainable Chem. Eng.*, 2020, **8**, 18889–18902.
20 A. L. Garay, A. Pichon and S. L. James, *Chem. Soc. Rev.*, 2007, **36**, 846–855.
21 S. B. Norbert Stock, *Chem. Rev.*, 2011, 933–969.
22 T. Stolar and K. Užarević, *CrystEngComm*, 2020, **22**, 4511–4525.
23 G. Ayoub, B. Karadeniz, A. J. Howarth, O. K. Farha, I. Lilović, L. S. Germann, R. E. Dinnebier, K. Užarević and T. Friščić, *Chem. Mater.*, 2019, **31**, 5494–5501.
24 C. Mottillo and T. Friščić, *Molecules*, 2017, **22**, 1–38.
25 D. Braga, F. Grepioni, L. Maini, P. P. Mazzeo and B. Ventura, *New J. Chem.*, 2011, **35**, 339–344.
26 D. Braga, S. L. Giaffreda, F. Grepioni and M. Polito, *CrystEngComm*, 2004, **6**, 458–462.
27 L. Maini, D. Braga, P. P. Mazzeo and B. Ventura, *Dalton Trans.*, 2012, **41**, 531–539.
28 F. Grifasi, M. R. Chierotti, C. Garino, R. Gobetto, E. Priola, E. Diana and F. Turci, *Cryst. Growth Des.*, 2015, **15**, 2929–2939.
29 G. A. Bowmaker, N. Chaichit, C. Pakawatchai, B. W. Skelton and A. H. White, *J. Chem. Soc. Dalton Trans.*, 2008, 2926–2928.
30 G. Scholz, S. Breitfeld, T. Krahl, A. Düvel, P. Heitjans and E. Kemnitz, *Solid State Sci.*, 2015, **50**, 32–41.
31 D. Prochowicz, M. Franckevičius, A. M. Cieślak, S. M. Zakeeruddin, M. Grätzel and J. Lewiński, *J. Mater. Chem. A*, 2015, **3**, 20772–20777.
32 A. D. Jodlowski, A. Yépez, R. Luque, L. Camacho and G. de Miguel, *Angew. Chem., Int. Ed.*, 2016, **55**, 14972–14977.
33 L. Maini, P. P. Mazzeo, F. Farinella, V. Fattori and D. Braga, *Faraday Discuss.*, 2014, **170**, 93–107.
34 G. A. Bowmaker, N. Chaichit, C. Pakawatchai, B. W. Skelton and A. H. White, *Dalton Trans.*, 2008, 2926–2928.
35 M. F. Thorne, M. L. R. Gómez, A. M. Bumstead, S. Li and T. D. Bennett, *Green Chem.*, 2020, **22**, 2505–2512.
36 P. A. Julien, K. Užarević, A. D. Katsenis, S. A. J. Kimber, T. Wang, O. K. Farha, Y. Zhang, J. Casaban, L. S. Germann, M. Etter, R. E. Dinnebier, S. L. James, I. Halasz and T. Friščić, *J. Am. Chem. Soc.*, 2016, **138**, 2929–2932.
37 A. A. L. Michalchuk and F. Emmerling, *Angew. Chem., Int. Ed.*, 2022, **61**, 1–14.
38 M. Wilke, L. Batzdorf, F. Fischer, K. Rademann and F. Emmerling, *RSC Adv.*, 2016, **6**, 36011–36019.
39 E. Izak-Nau, D. Campagna, C. Baumann and R. Göstl, *Polym. Chem.*, 2020, **11**, 2274–2299.
40 G. A. Bowmaker, *Chem. Commun.*, 2013, **49**, 334–348.
41 R. T. O'Neill and R. Boulatov, *Nat. Rev. Chem.*, 2021, **5**, 148–167.
42 K. Linberg, B. Röder, D. Al-Sabbagh, F. Emmerling and A. A. L. Michalchuk, *Faraday Discuss.*, 2022, **241**, 178–193.
43 C. Zuffa, C. Cappuccino, M. Marchini, L. Contini, F. Farinella and L. Maini, *Faraday Discuss.*, 2023, **241**, 448–465.
44 C. Cappuccino, F. Farinella, D. Braga and L. Maini, *Cryst. Growth Des.*, 2019, **19**, 4395–4403.
45 E. Kwon, J. Kim, K. Y. Lee, T. H. Kim, K. Yeol Lee and T. Ho Kim, *Inorg. Chem.*, 2017, **56**, 943–949.
46 J. Conesa-Egea, F. Zamora and P. Amo-Ochoa, *Coord. Chem. Rev.*, 2019, **381**, 65–78.
47 E. Kwon, J. Kim, K. Y. Lee and T. H. Kim, *Inorg. Chem.*, 2017, **56**, 943–949.
48 J. Conesa-Egea, J. Gallardo-Martínez, S. Delgado, J. I. Martínez, J. Gonzalez-Platas, V. Fernández-Moreira, U. R. Rodríguez-Mendoza, P. Ocón, F. Zamora and P. Amo-Ochoa, *Small*, 2017, **13**, 1700965.
49 A. Kobayashi and M. Kato, *Chem. Lett.*, 2017, **46**, 154–162.
50 J.-J. Liu, Y. Chen, M.-J. Lin, C.-C. Huang and W.-X. Dai, *Dalton Trans.*, 2016, **45**, 6339–6342.
51 N. M. Khatri, M. H. Pablico-Lansigan, W. L. Boncher, J. E. Mertzman, A. C. Labatete, L. M. Grande, D. Wunder, M. J. Prushan, W. Zhang, P. S. Halasyamani, J. H. S. K. Monteiro, A. de Bettencourt-Dias, S. L. Stoll, P. Shiv Halasyamani, J. HSK Monteiro, A. de Bettencourt-Dias and S. L. Stoll, *Inorg. Chem.*, 2016, **55**, 11408–11417.
52 J. Troyano, O. Castillo, J. I. Martínez, V. Fernández-Moreira, Y. Ballesteros, D. Maspoch, F. Zamora and S. Delgado, *Adv. Funct. Mater.*, 2018, **28**, 1704040.

53 J. Conesa-Egea, C. D. Redondo, J. I. Martínez, C. J. Gómez-García, Ó. Castillo, F. Zamora and P. Amo-Ochoa, *Inorg. Chem.*, 2018, **57**, 7568–7577.
54 J. Conesa-Egea, N. Nogal, J. I. Martínez, V. Fernández-Moreira, U. R. Rodríguez-Mendoza, J. González-Platas, C. J. Gómez-García, S. Delgado, F. Zamora and P. Amo-Ochoa, *Chem. Sci.*, 2018, **9**, 8000–8010.
55 B. Xin, J. Sang, Y. Gao, G. Li, Z. Shi and S. Feng, *RSC Adv.*, 2018, **8**, 1973–1978.
56 S. Sugimoto, H. Ohtsu and K. Tsuge, *J. Photochem. Photobiol. A Chem.*, 2018, **353**, 602–611.
57 A. Kobayashi, Y. Yoshida, M. Yoshida and M. Kato, *Chem. – A Eur. J.*, 2018, **24**, 14750–14759.
58 H. Park, E. Kwon, H. Chiang, H. Im, K. Y. Lee, J. Kim and T. H. Kim, *Inorg. Chem.*, 2017, **56**, 8287–8294.
59 S. S.-Q. Bai, K. L. Ke, D. J. Young and T. S. A. Hor, *J. Organomet. Chem.*, 2017, 137–141.
60 L. Maini, D. Braga, P. P. Mazzeo, L. Maschio, M. Rerat, I. Manet and B. Ventura, *Dalton Trans.*, 2015, **44**, 13003–13006.
61 A. H. Johnstone, *J. Chem. Technol. Biotechnol.*, 2007, **50**, 294–295.
62 H. Schmidbaur and A. Schier, *Angew. Chem., Int. Ed.*, 2015, **54**, 746–784.
63 G. M. Sheldrick, *Acta Crystallogr., Sect. A: Found. Crystallogr.*, 2015, **71**, 3–8.
64 R. Herbst-Irmer and G. M. Sheldrick, *Int. Union Crystallogr. Acta Crystallogr. Sect. B Acta Cryst.*, 1998, **54**, 443–449.
65 A. A. Coelho, *J. Appl. Crystallogr.*, 2018, **51**, 210–218.
66 C. F. MacRae, I. Sovago, S. J. Cottrell, P. T. A. Galek, P. McCabe, E. Pidcock, M. Platings, G. P. Shields, J. S. Stevens, M. Towler and P. A. Wood, *J. Appl. Crystallogr.*, 2020, **53**, 226–235.
67 T. Degen, M. Sadki, E. Bron, U. König and G. Nénert, *Powder Diffr.*, 2014, **29**, S13–S18.
68 Zizak, *Journal of large-scale research facilities*, 2016, DOI: **10.17815/jlsrf-2-113**.
69 G. I. Lampronti, A. A. L. Michalchuk, P. P. Mazzeo, A. M. Belenguer, J. K. M. Sanders, A. Bacchi and F. Emmerling, *Nat. Commun.*, 2021, **12**, 1–9.
70 G. Benecke, W. Wagermaier, C. Li, M. Schwartzkopf, G. Flucke, R. Hoerth, I. Zizak, M. Burghammer, E. Metwalli, P. Müller-Buschbaum, M. Trebbin, S. Förster, O. Paris, S. V. Roth and P. Fratzl, *J. Appl. Crystallogr.*, 2014, **47**, 1797–1803.
71 R. Meijboom, R. J. Bowen and S. J. Berners-Price, *Coord. Chem. Rev.*, 2009, **253**, 325–342.
72 N. K. Mills and A. H. White, *J. Chem. Soc. Dalton Trans.*, 1984, 225–228.
73 C. R. Groom, I. J. Bruno, M. P. Lightfoot and S. C. Ward, *Acta Crystallogr. Sect. B Struct. Sci. Cryst. Eng. Mater.*, 2016, **72**, 171–179.